Optimization of Pr3+, Tb3+, and Sm3+ co-doped (Y0.65Gd0.35)BO3:Eu0.05(3+) VUV phosphors through combinatorial approach.

ARTICLE *in* JOURNAL OF COMBINATORIAL CHEMISTRY · SEPTEMBER 2008

Impact Factor: 4.93 · Source: PubMed

5 AUTHORS, INCLUDING:

Lei Chen
Hefei University of Technology
58 PUBLICATIONS **592** CITATIONS
SEE PROFILE

Guobin Zhang
University of Science and Technology of C…
82 PUBLICATIONS **1,094** CITATIONS
SEE PROFILE

Optimization of Pr^{3+}, Tb^{3+}, and Sm^{3+} Co-Doped $(Y_{0.65}Gd_{0.35})BO_3:Eu_{0.05}^{3+}$ VUV Phosphors through Combinatorial Approach

Lei Chen,† Yibing Fu, Guobin Zhang, Jun Bao, and Chen Gao*

National Synchrotron Radiation Laboratory & Department of Physics, University of Science & Technology of China, Hefei, Anhui 230026, China

Received October 28, 2007

A combinatorial approach was used to systematically investigate the effect of trace Pr^{3+}, Tb^{3+}, or Sm^{3+} on the VUV photoluminescence of Eu^{3+} in the Pr^{3+}, Tb^{3+}, or Sm^{3+} co-doped $(Y_{0.65}Gd_{0.35})BO_3:Eu^{3+}_{0.05}$. We found that Pr^{3+} and Tb^{3+}increases the VUV photoluminescent efficiency, while Sm^{3+} decreases the efficiency. The optimized composition was identified to be between 7×10^{-6} and 3×10^{-4}, and the corresponding efficiency improvement is about 15%. Scale-up experiments confirmed the results in the combinatorial materials libraries.

Introduction

Driven by the advances in the plasma display panel (PDP) and Hg-free fluorescent lamps, the demand for high-efficiency vacuum ultraviolet (VUV) phosphors increases significantly. Recently, the dominant PDP red phosphors are $(Y,Gd)BO_3:Eu^{3+}$ and $Y_2O_3:Eu^{3+}$. A major drawback of these phosphors is low efficiency.[1] To achieve the desirable luminance of 700 cd/m^2 for high-definition television display, the luminescent efficiency of PDP phosphors must be improved from present 1–1.5 lm/w to above 5 lm/w.[2,3] Such a big advancement needs a series of improvements on both the VUV phosphors and the discharge technique. Although many researchers have worked on the improvement of the Eu^{3+}-activated borate,[4,5] phosphate,[2] aluminate,[6] silicate,[7] vanadate,[8] oxide,[9] fluoride,[10] and their composites[11–14] through co-doping, few phosphors with efficiency higher than $(Y,Gd)BO_3:Eu^{3+}$ were reported.

One of the key factors which influence the photoluminescent efficiency is the energy-transfer process from the host to activator.[15] This transfer could be strongly affected by the defects (carrier traps) in the host material. From this point of view, trace co-dopant with different affinity has the potential to change the trap configuration and consequently to improve the efficiency significantly. A successful example is the Pr^{3+}, Tb^{3+} in $Y_2O_2S:Eu^{3+}$ under cathode ray excitation.[16,17] However, the transfer process depends strongly on the type, valence, and density of the co-doped impurities. Systematic investigation on the effect of co-dopants is extremely time-consuming.

In this paper, the combinatorial approach, which has been successfully applied to search for new PDP phosphors,[18] was adopted to systematically study the effect of Pr^{3+}, Tb^{3+}, and Sm^{3+} co-dopants on the VUV photoluminescence of $(Y_{0.65}Gd_{0.35})BO_3:Eu^{3+}_{0.05}$. We found that trace Pr^{3+} and Tb^{3+} increases the VUV photoluminescent efficiency of $(Y_{0.65}Gd_{0.35})BO_3:Eu^{3+}_{0.05}$ by a factor of ~15%.

Experimental Section

The starting materials were Y_2O_3 (99.99%), Gd_2O_3 (99.99%), Eu_2O_3 (99.99%), H_3BO_3 (99.5%), Pr_6O_{11} (99.99%), Tb_4O_{11} (99.99%), and Sm_2O_3 (99.99%), oxalic acid (analytic reagent (A.R.)), nitric acid (A.R.), and ethanol (A.R.). To increase the amount of materials synthesized in the microreactors, suspension precursors were used for host as described in ref 19, while precursors for dopants were in nitrate aqueous solution to keep the small composition step controllable. The synthesis of the libraries is similar to our previous report (ref 20). In the synthesis, H_3BO_3 was provided in a stoichiometric 20 mol % excess to compensate for evaporation in the post-annealing step. The as-deposited libraries were first solvent evaporated in an ambient air environment, then heated at 176 °C, which is the melting point for H_3BO_3, for 30 min to allow the diffusion of H_3BO_3, annealed at 900 °C for 120 min, and finally sintered at 1150 °C for 180 min.

To characterize the VUV photoluminescence, an imaging system was developed as shown in Figure 1. A RF powdered Xe spectrum lamp (model no. XeLM-L, Resonance Ltd.), which simulates the discharge radiation in the PDP and Hg-free lamp, was used as the excitation light source. The 147 nm emission was incident on the library, and the VUV photoluminescent intensity of the materials in the library was recorded using a digital CCD camera through the optical window. The sample chamber was evacuated to remove the air absorption on VUV radiation.

To calibrate the uneven illumination of the pointlike source, the VUV photoluminescence image of a "standard library" (the predrilled holes of a library substrate were manually filled with the same amount of a commercial PDP

* To whom correspondence should be addressed. E-mail: cgao@ustc.edu.cn.
† Current address: School of Materials Science and Engineering, Hefei University of Technology, Hefei, Anhui 230009, China.

10.1021/cc700172e CCC: $40.75
Published on Web 03/13/2008

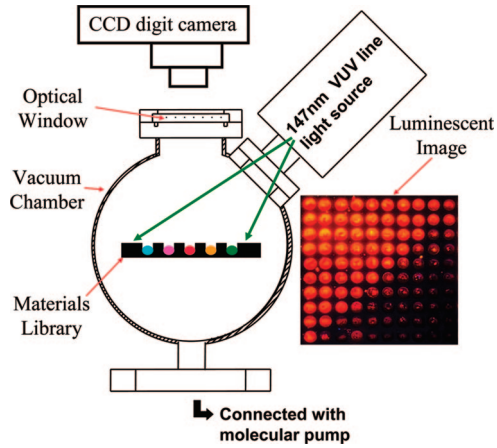

Figure 1. Schematic diagram of the VUV photoluminescence imaging system.

red phosphor (Y,Gd)BO_3:Eu^{3+}, obtained from the Grirem Advanced Materials Co., Ltd.) was taken first. Because the photoluminescence efficiency of all the sample sites is the same, the relative brightness as the function of position on the image reflects the illumination intensity distribution quantitatively. Then, the calibrated photoluminescent intensity is obtained by division of the raw intensity on the image by the distribution. To estimate the intrinsic error of the system, another standard library was made. The standard deviation of its calibrated photoluminescent intensity is calculated to be <1%.

Results and Discussion

A luminescent photograph obtained under 147 nm VUV excitation of the Pr^{3+}, Tb^{3+}, and Sm^{3+} co-doped $(Y_{0.65}Gd_{0.35})BO_3:Eu^{3+}_{0.05}$ libraries is shown in Figure 2a, together with the composition map. To clearly display the variation, the calibrated luminescent intensities as the functions of composition are also plotted in Figure 2a. From the figure, we found that the intensities increase with Pr^{3+} or Tb^{3+} concentration at first and then rapidly decrease when the concentration exceed 7.5×10^{-4}. The Sm^{3+} co-doped samples do not show the enhancement effect.

To zoom in on the peak intensity region, a secondary Pr^{3+} and Tb^{3+} co-doped $(Y_{0.65}Gd_{0.35})BO_3:Eu^{3+}_{0.05}$ library that covers the composition range from 3×10^{-6} to 3×10^{-4} with smaller composition steps was synthesized, and its 147 nm VUV photoluminescent photograph and calibrated luminescent intensities are shown in Figure 2b. The highest VUV photoluminescent composition is between 7×10^{-6} and 3×10^{-4}.

To confirm the above results and quantify the VUV photoluminescence enhancement, scale-up samples for the un-doped $(Y_{0.65}Gd_{0.35})BO_3:Eu^{3+}_{0.05}$ and 1×10^{-4} Pr^{3+} or Tb^{3+} co-doped $(Y_{0.65}Gd_{0.35})BO_3:Eu^{3+}_{0.05}$ were synthesized through solid-state reaction under the same conditions: Un-doped/co-doped $(Y_{0.65}Gd_{0.35})_2O_3:Eu^{3+}_{0.05}$ oxides were prepared by sintering their coprecipitated oxalates at 1000 °C for 120 min; then these oxides were wet ball-milled with a stoichiometric 10 mol % excess of H_3BO_3 in additive ethanol. The ball-milled mixtures were sintered at 600 °C for 120 min and ground in an agate mortar. Then, these mixtures were annealed at 900 °C for 120 min and sintered at 1200 °C for 180 min. Finally, the fired products were wet ball-milled in deionized water and washed with 80–100 °C deionized water several times to remove excess B_2O_3 and dried at 120 °C.

The microstructure of different doped samples was analyzed using XRD and SEM, and no significant difference was found in the XRD patterns and SEM micrographs. Typical XRD patterns and SEM micrograph are given in Figure 3, which shows that all the scale-up samples were well crystallized into hexagonal YBO_3 (JCPDS card 74-1929) structure and that the enhancement is not from the difference in the morphology of the grain.

The VUV excitation and emission spectra of the scale-up samples were measured at NSRL VUV spectroscopy endstation on U24 beamline. Detailed description on the measurements can be found in our previous work.[21]

The emission spectra of the scale-up samples under 147 nm excitation are shown in Figure 4, in which all samples exhibit almost the same emission configuration. So the chromaticity of the co-doped $(Y_{0.65}Gd_{0.35})BO_3:Eu^{3+}_{0.05}$ should be the same as that of $(Y_{0.65}Gd_{0.35})BO_3:Eu^{3+}_{0.05}$, which is (0.65,0.35).[22] No characteristic emission from Pr^{3+} or Tb^{3+} was observed. The relative VUV photoluminescent intensity of 1×10^{-4} Pr^{3+} or Tb^{3+} co-doped $(Y_{0.65}Gd_{0.35})BO_3:Eu^{3+}_{0.05}$ integrated from 584 to 633 nm is about 14% or 15% higher than that of the un-doped $(Y_{0.65}Gd_{0.35})BO_3:Eu^{3+}_{0.05}$, respectively. We also compared the intensity of our co-doped $(Y_{0.65}Gd_{0.35})BO_3:Eu^{3+}_{0.05}$ with the commercial PDP red phosphor obtained from the Grirem Advanced Materials Co., Ltd., and found that ~7% enhancement is achieved. This result indicates that there is ~8% efficiency difference between the commercial (Y,Gd)BO_3:Eu^{3+} and our un-doped $(Y_{0.65}Gd_{0.35})BO_3:Eu^{3+}_{0.05}$. This is a reasonable result because the grain morphology from the solid-state reaction is usually irregular.[23] Considering that there could be ~20% efficiency improvement through grain morphology control,[24] our ~15% efficiency enhancement estimation is quite conservative.

The excitation spectra of the Eu^{3+} emission at 592 nm of the scale-up samples are shown in Figure 5. They all have the same configuration. The bands with absorption edges at 170 and 223 nm are attributed to the band gap absorption of host lattice (HB) and $O^{2-} \rightarrow Eu^{3+}$ changer-transfer absorption (CTB), respectively. The excitation lines at 274 and 276 nm are assigned to the $^8S_{7/2} \rightarrow {}^6I_J$ transition of Gd^{3+}. The characteristic absorption of Pr^{3+} and Tb^{3+} is not observed in the excitation spectra, which indicates that the energy transfer from Pr^{3+}/Tb^{3+} to Eu^{3+} through the resonance or exchange effect does not exist.

Because the significant enhancement occurs at the trace (3×10^{-6}–3×10^{-4}) Pr^{3+} or Tb^{3+} co-doping level, it is hard to account for it using the traditional sensitization mechanism, which requires a relatively high sensitizer concentration for the resonant energy transfer from the sensitizer to the luminescent center. We believe that this enhancement is caused by modification of the trap configuration. A similar effect has been reported in cathode luminescence where ~230% efficiency enhancement was found in $Y_2O_2S:Eu^{3+}$ through trace doping of Pr^{3+} and

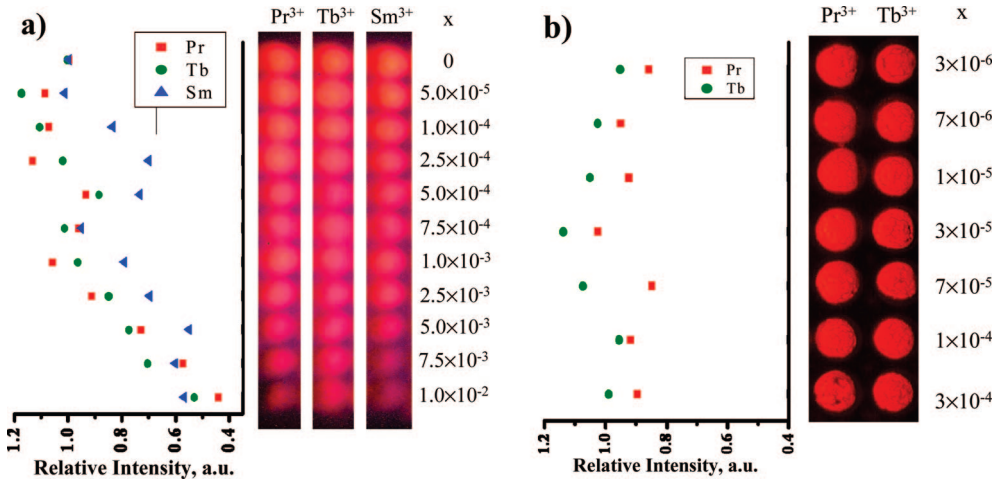

Figure 2. Composition maps, VUV photoluminescence photographs, and the calibrated photoluminescent intensities as the functions of composition of the (a) primary and (b) secondary combinatorial libraries at 147 nm excitation: red square, Pr^{3+} co-doped $(Y_{0.65}Gd_{0.35})BO_3:Eu^{3+}_{0.05}$; green circle, Tb^{3+} co-doped $(Y_{0.65}Gd_{0.35})BO_3:Eu^{3+}_{0.05}$; blue triangle, Sm^{3+} co-doped $(Y_{0.65}Gd_{0.35})BO_3:Eu^{3+}_{0.05}$.

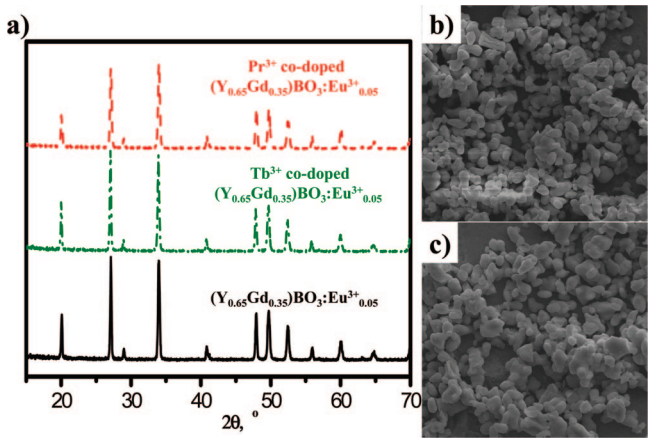

Figure 3. (a) XRD patterns of 1×10^{-4} Pr^{3+} (red dashed line), Tb^{3+} co-doped $(Y_{0.65}Gd_{0.35})BO_3:Eu^{3+}_{0.05}$ (green dashed-dotted line), and $(Y_{0.65}Gd_{0.35})BO_3:Eu_{0.05}$ (black solid line); (b) SEM micrograph of Pr^{3+} co-doped $(Y_{0.65}Gd_{0.35})BO_3:Eu^{3+}_{0.05}$; (c) SEM micrograph of $(Y_{0.65}Gd_{0.35})BO_3:Eu^{3+}_{0.05}$.

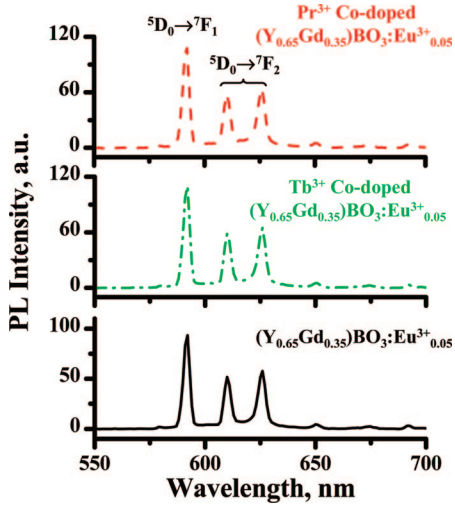

Figure 4. Emission spectra of Pr^{3+} (red dash line) and Tb^{3+} co-doped (green dashed-dotted line) $(Y_{0.65}Gd_{0.35})BO_3:Eu^{3+}_{0.05}$ and $(Y_{0.65}Gd_{0.35})BO_3:Eu^{3+}_{0.05}$ (black solid line).

Tb^{3+}.[17] Upon absorption of VUV photons, electrons are generated in the conduction band, and holes are left in the valance band. These photoproduced carriers migrate in the

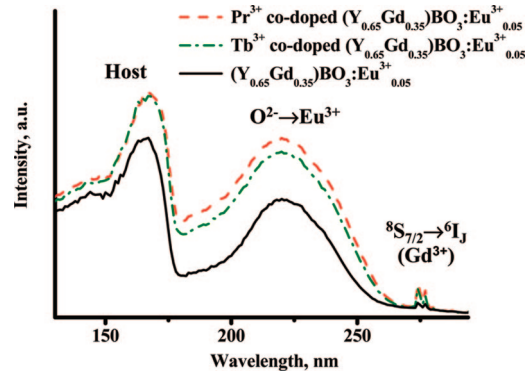

Figure 5. Excitation spectra of Pr^{3+} (red dashed line), Tb^{3+} co-doped (green dashed-dotted line) $(Y_{0.65}Gd_{0.35})BO_3:Eu^{3+}_{0.05}$, and $(Y_{0.65}Gd_{0.35})BO_3:Eu^{3+}_{0.05}$ (black solid line).

host lattice. Photoluminescence takes place when Eu^{3+} captures an electron–hole pair. Because of the large electronegativity, Eu^{3+} and Sm^{3+} are good electron traps. Unfortunately, holes have a large probability of being captured by native defects, namely, O^{2-} vacancies. Because Pr^{3+} and Tb^{3+} show relatively strong reduction trends, doping with Pr^{3+} or Tb^{3+} adds shallow hole traps. These shallow traps compete with O^{2-} vacancy for the capture of the photoproduced holes. However, because the holes captured in the shallow traps have a large probability of thermal release, it increases the hole capture probability of Eu^{3+}. On the other hand, doping with Sm^{3+} introduces a competing center for the capture of electrons with Eu^{3+}. Further investigation on the energy transfer process is currently underway.

Conclusion

In conclusion, the effect of trace Pr^{3+}, Tb^{3+}, or Sm^{3+} on the VUV photoluminescence of $(Y_{0.65}Gd_{0.35})BO_3:Eu^{3+}_{0.05}$ was systematically investigated. Pr^{3+} and Tb^{3+} are found to have positive effects on the VUV photoluminescence of $(Y_{0.65}Gd_{0.35})BO_3:Eu^{3+}_{0.05}$, and the optimal composition is identified to be between 7×10^{-6} and 3×10^{-4}. Scale-up experiments confirmed the results from the combinatorial method and also determined that the efficiency improvement is ~15%.

Acknowledgment. This work was financed by NSFC (50421201).

References and Notes

(1) Kim, C.-H.; Kwon, I.-E.; Park, C.-H.; Hwang, Y.-J.; Bae, H.-S.; Yu, B.-Y.; Pyun, C.-H.; Hong, G.-Y. *J. Alloys Compd.* **2000**, *311*, 33–39.
(2) Rao, R. P.; Devine, D. J. *J. Lumin.* **2000**, *87–89*, 1260–1263.
(3) Liu, X.; Wang, X.; Xie, Y.; Ma, L.; Zhang, X. *Chin. J. Liq. Cryst. Displays* **1998**, *13* (3), 155–162.
(4) Park, W.; Summers, C. J.; Do, Y. R.; Yang, H. G. J. *Mater. Sci.* **2002**, *37*, 4041–4045.
(5) Wei, Z.; Sun, L.; Liao, C.; Yan, C. *Appl. Phys. Lett.* **2002**, *80*, 1447–1449.
(6) Wang, Y.; Endo, T.; Li, F. J. *Rare Earth* **2004**, *22*, 95–99.
(7) Chen, Y.; Liu, B.; Shi, C.; Kirm, M.; True, M.; Vielhauer, S.; Zimmerer, G. *J. Phys.: Condens. Matter* **2005**, *17*, 1217–1224.
(8) Zhang, Q.-L.; Guo, C.-X.; Shi, C.-S.; Wei, Y.-G.; Qi, Z.-M.; Tao, Y. *J. Chin. Rare Earth Soc.* **2001**, *19*, 1–4.
(9) Kim, E. J.; Kang, Y. C.; Park, H. D.; Ryu, S. K. *Mater. Res. Bull.* **2003**, *38*, 515–524.
(10) Hirai, T.; Ohno, N.; Hashimoto, S.; Sakuragi, S. *J. Alloys Compd.* **2006**, *408–412*, 894–897.
(11) Tian, L.; Yu, B.-Y.; Pyun, C.-H.; Park, H. L.; Mho, S.-I. *Solid State Commun.* **2004**, *129*, 43–46.
(12) Liang, H.; Zeng, Q.; Tao, Y.; Wang, S.; Su, Q. *Mater. Sci. Eng. B* **2003**, *98*, 213–219.
(13) Zeng, X.-Q.; Hong, G.-Y.; You, H.-P.; Wu, X.-Y.; Kim, C.-H.; Yun, C.-H.; Yu, B.-Y.; Bae, H.-S.; Park, C.-H.; Kwon, I.-E.; Chin, *J. Lumin.* **2001**, *22*, 55–58.
(14) Wang, Y.; Endo, T.; Xie, E.; He, D.; Liu, B. *Microelectron. J.* **2004**, *35*, 357–361.
(15) Yamamoto, H.; Urade, K. *J. Electrochem. Soc.* **1982**, *129* (9), 2069–2074.
(16) Kano, T. In *Phosphor Handbook*; Shionoya, S., Yen, W. M.; CRC Press: Boca Raton, FL, 2000; p 185.
(17) Yamamoto, H.; Kano, T. *J. Electrochem. Soc.* **1979**, *126* (2), 305–312.
(18) (a) Sohn, K.-S.; Kim, C. H.; Park, J. T.; Park, H. D. *J. Mater. Res.* **2002**, *17* (12), 3201–3205. (b) Sohn, K.-S.; Zeon, I. W.; Chang, H.; Lee, S. K.; Park, H. D. *Chem. Mater.* **2002**, *14*, 2140–2148. (c) Kim, C. H.; Park, S. M.; Park, J. K.; Park, H. D.; Sohn, H.-S.; Park, J. T. *J. Electrochem. Soc.* **2002**, *149* (12), H183–H187. (d) Sohn, K.-S.; Lee, J. M.; Jeon, I. W.; Park, H. D. *J. Electrochem. Soc.* **2003**, *150* (8), H182–H186. (e) Sohn, K.-S.; Yoo, J. G.; Shin, N.; Toda, K.; Zang, D. S. *J. Electrochem. Soc.* **2005**, *152* (12), H213–H218.
(19) Chen, L.; Liu, Z.-H.; Shen, L.; Bao, J.; Liu, W.-H.; Gao, C. *Acta Phys. Sin.* **2004**, *20* (7), 722–726.
(20) Chen, L.; Bao, J.; Gao, C.; Huang, S.; Liu, C.; Liu, W. *J. Comb. Chem.* **2004**, *6*, 699–702.
(21) Gao, C.; Chen, L.; Bao, J.; Fu, Y.; Zhang, G. *J. Electrochem. Soc.* **2007**, *154* (11), J345–347.
(22) Kojima, T. In *Phosphor Handbook*; Shionoya, S., Yen, W. M.; CRC Press: Boca Raton, FL, 2000; p 633.
(23) Kim, D.-S.; Lee, R.-Y. *J. Mater. Sci.* **2000**, *35* (19), 4777–4782.
(24) Jeoung, B. W.; Hong, G. Y.; Yoo, W. T.; Yoo, J. S. *J. Electrochem. Soc.* **2004**, *151* (10), H213–H216.

CC700172E